Pressure-induced charge density wave phase in $Ag_{2-\delta}Te$

Yongsheng Zhao,[1] Wenge Yang,[1,*] Harold S. Schnyders,[2] Anke Husmann,[3] Ganghua Zhang,[1] Yang Ren,[4] David L. Price,[5] Ho-Kwang Mao,[1,6] and Marie-Louise Saboungi[7,†]

[1]*Center for High Pressure Science and Technology Advanced Research (HPSTAR), 1690 Cailun Road, Shanghai 201203, People's Republic of China*

[2]*Physics Department, Grand Valley State University, Allendale, Michigan 49401, USA*

[3]*Department of Materials Science and Metallurgy, University of Cambridge, 27 Charles Babbage Road, Cambridge CB3 0FS, United Kingdom*

[4]*X-Ray Science Division, Advanced Photon Source, Argonne National Laboratory, 9700 S. Cass Avenue, Argonne, Illinois 60439, USA*

[5]*CEMHTI, UPR 3079 CNRS - Université d'Orléans, 1d Avenue de la Recherche Scientifique, 45071 Orléans Cedex 2, France*

[6]*Geophysical Laboratory, Carnegie Institution of Washington, Washington, DC 20015, USA*

[7]*IMPMC, UMR 7590 CNRS - Sorbonne Université, Campus Pierre et Marie Curie, 4 Place Jussieu, 75252 Paris Cedex 5, France*

(Received 1 April 2018; published 15 November 2018)

Considerable excitement was generated by the observation of large and linear positive magnetoresistance in nonmagnetic silver chalcogenides. Renewed interest in these materials was kindled by the discovery that Ag_2Te in particular is a topological insulator with gapless linear Dirac-type surface states. High-pressure x-ray-diffraction studies, combined with first-principles electronic structure calculations, have identified three phase transitions as the pressure is increased: an isostructural transition identified with an electronic topological transition followed by two structural phase transitions. These recent studies were carried out on nominally stoichiometric Ag_2Te. For the present work we have prepared single-phase self-doped $Ag_{2-\delta}Te$ samples with a well-characterized silver deficit ($\delta = 2.0\times10^{-4}$) for structural and electrical transport measurements over extended ranges of pressure (0–43 GPa), temperature (2–300 K), and magnetic field (0–9 T). The temperature dependence of the resistivity exhibits anomalous behavior at 2.3 GPa, slightly above the isostructural transition, which we postulate is due to Fermi surface reconstruction associated with a charge density wave (CDW) phase. The anomaly is enhanced by the application of a 9-T magnetic field and shifted to higher temperature, implying that the electronic Zeeman energy is sufficient to alter the gapping of the Fermi surface. A peak in the pressure dependence of the resistivity and a sudden drop in the pressure dependence of the mobility, occurring at 2.3 GPa, provide additional evidence for a CDW phase at pressures slightly above the isostructural transition.

DOI: 10.1103/PhysRevB.98.205126

I. INTRODUCTION

The nonmagnetic silver chalcogenides display many fascinating phenomena including fast-ion conduction at higher temperatures and a linear magnetoresistance (MR) in fields ranging from 10^{-3} to 5.5 T, without any sign of saturation, in $Ag_{2+\delta}Se$ and $Ag_{2+\delta}Te$ with $\delta \sim 0.01$ [1]. Subsequent work demonstrated that the linear MR extended over a range of carrier densities in both Ag-rich and Ag-deficient materials [2], maintained a linear dependence on magnetic field without saturation up to 60 T [3], and could be enhanced by tuning the band gap with applied pressure [4]. More recently it was suggested that Ag_2Te in particular is a topological insulator with gapless linear Dirac-type surface states [5], and that this might explain the unusual MR behavior without invoking a minority metallic phase, which formed the basis of earlier quantum [6] and classical [7] explanations of the phenomenon. Topological surface states have been subsequently confirmed experimentally [8,9]. This work was followed by several high-pressure x-ray-diffraction studies combined with first-principles electronic structure calculations, identifying four phases as the pressure is increased [10–12]. Phase I was determined to be semiconducting with topological conducting surface states, transforming into a semimetallic phase II through an isostructural transition identified as an electronic topological transition at 1.8–2.0 GPa. This is followed by structural transitions to metallic phases III and IV. The recent measurements of transport properties under pressure by Zhang *et al.* [11] and Zhu *et al.* [12] showed a collapse of the resistivity at the isostructural transition, while the temperature dependence confirmed a semiconducting behavior up to [11] or slightly beyond [12] the isostructural transition and fully metallic beyond it. At low pressures the MR has a quadratic dependence on temperature followed by linear dependence without saturation, changing to purely quadratic as the pressure is increased [12].

It should be noted that the recent experimental studies and first-principles calculations were carried out on nominally stoichiometric Ag_2Te, and the theoretical work assumed that the effect of doping was to shift the Fermi level through the rigid band structure, without consideration of defect states within the gap. In the present work, we take advantage of

*yangwg@hpstar.ac.cn
†marie-louise.saboungi@sorbonne-universite.fr

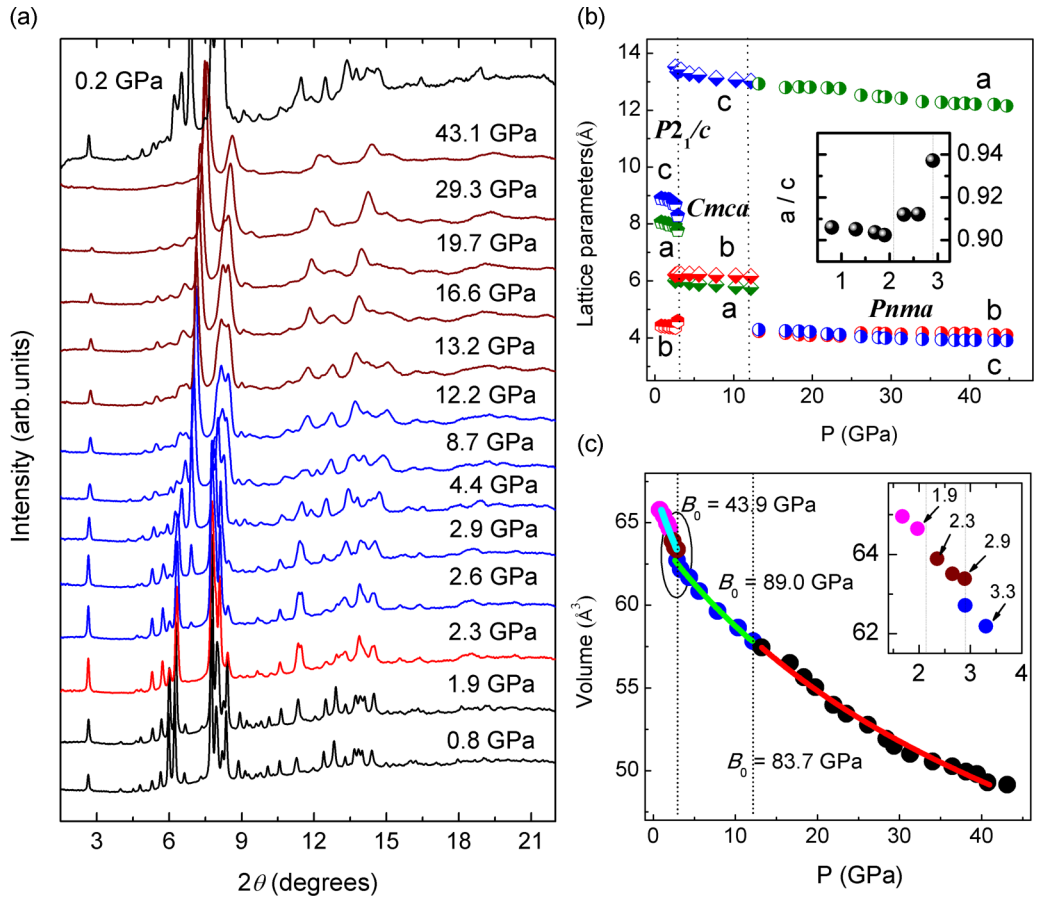

FIG. 1. (a) Angle-dispersive XRD patterns of $Ag_{2-\delta}Te(\delta = 2\times10^{-4})$ at selected pressures. (b) Lattice parameters as a function of pressure obtained from Rietveld refinement, showing the jump at the phase transition from $P2_1/c$ to *Cmca* at 2.9 GPa and then to *Pnma* around 12.9 GPa. The inset shows the change of a/c with pressure, with discontinuities at the isostructural transition around 2.1 GPa and at the $P2_1/c \rightarrow Cmca$ transition at 2.9 GPa. (c) Unit-cell volume obtained from Rietveld refinement as a function of pressure. The solid curves represent fits of the second-order Birch-Murnaghan equation. The inset shows an enlarged plot of the low-pressure region, in which the unit-cell volume is discontinuous around 2.1 GPa due to the isostructural transition and at 2.9 GPa due to the $P2_1/c \rightarrow Cmca$ transition, where the two phases coexist.

meticulous preparation of single-phase self-doped chalcogenides recently developed by Schnyders [13] to synthesize samples of $Ag_{2-\delta}Te$, $\delta = 2.0\times10^{-4}$, that are not only free of the secondary metallic phase assumed by the earlier theories but in addition have a well-characterized silver deficit. The value $\delta = 2.10^{-4}$ has been previously identified [14] as the silver deficit marking the doping boundary between 4 K extrinsic-regime p-type behavior at greater silver deficits and n-type behavior. As such, samples doped to this deficit have a Fermi energy located very near the conduction band edges and are optimally sensitive to changes caused by pressure.

We report here x-ray-diffraction and electrical-transport measurements on these samples over extended ranges of pressure: 0–43 GPa, temperature: 2–300 K, and magnetic field: 0–9 T.

A key discovery in this work is the observation of anomalous behavior of the temperature dependence of the resistivity at 2.3 GPa, slightly above the isostructural transition. We ascribe this behavior to Fermi surface reconstruction associated with a charge density wave (CDW) phase. The anomaly is enhanced by the application of a 9-T magnetic field and shifted to higher temperature, implying that the electronic Zeeman energy is sufficient to alter the gapping of the Fermi surface.

II. EXPERIMENTAL

A. Sample preparation

A slightly Te-rich mixture of 99.99% Ag and 99.9999% Te (Alfa Aesar) was sealed under vacuum in a quartz tube and simultaneously rocked and heated at 1000 °C for several hours before turning off the furnace. The samples under study were cut from pieces of the resulting boule that were processed in a $Ag/AgI/Ag_{2-\delta}Te$ electrochemical cell held at 200 °C in a simple laboratory-built fixture. These pieces were brought from as-prepared silver deficit into equilibrium with metallic silver ($\delta = 0$) by spontaneous flow of current, and subsequently reestablished at homogeneous silver deficit $\delta = 2^{*}10^{-4}$ with a cell voltage $V_{cell} = 90$ mV applied with a Keithley 6221 current supply [13,15]. Samples thus prepared were free of metallic inclusions. The dimensions of the sample used in these measurements were $0.15\times0.12\times0.04$ mm.

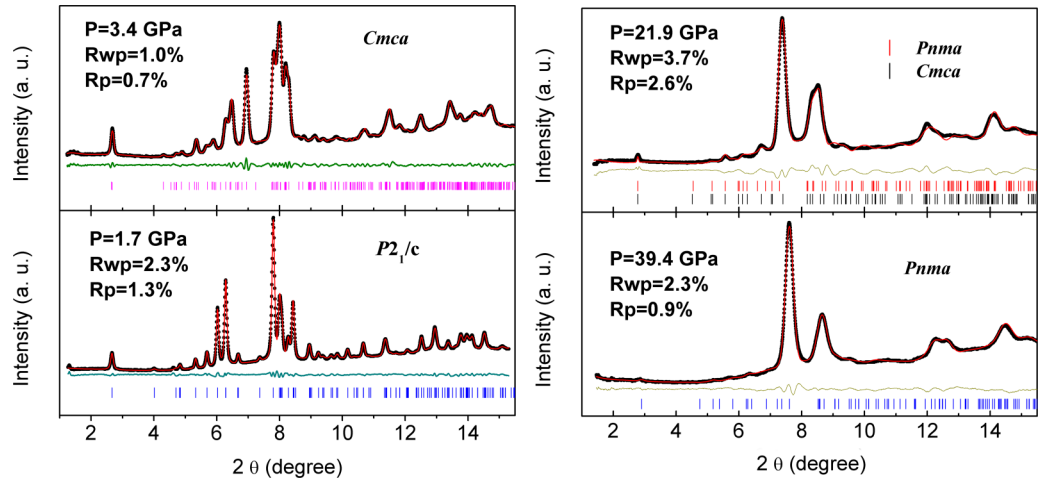

FIG. 2. Rietveld profile refinements of the XRD patterns at 1.7, 3.4, 21.9. and 39.4 GPa, representing the $P2_1/c$ phase, *Cmca* phase, coexisting *Cmca* and *Pnma* phases, and *Pnma* phase, respectively.

B. Measurements

The *in situ* high-pressure x-ray-diffraction experiments were performed at ambient temperature in the angle-dispersive synchrotron x-ray diffraction mode (AD-XRD) at beamline 16BM-D of the Advanced Photon Source, Argonne National Laboratory. Powder samples were loaded into a gasketed diamond-anvil cell (DAC) with a 16:3:1 methanol/ethanol/water mixture as a pressure-transmitting medium. Transport measurements were performed with the four-probe method on bar-shaped samples cut from polycrystalline ingots; those under magnetic field were made with the field perpendicular to the current direction. All investigations were carried out with a Quantum Design Physical Property Measurement System combined with an ac bridge in a DAC setup.

III. RESULTS AND DISCUSSION

A. Structure

The AD-XRD patterns at selected pressures shown in Fig. 1(a) display three transitions between 1.9 and 2.3 GPa, between 2.6 and 2.9 GPa, and between 12.2 and 13.2 GPa. Rietveld profile refinements (Fig. 2, left) at 1.7 and 3.4 GPa indicate $P2_1/c$ and *Cmca* phases, respectively, in accord with previous work [10–12]. The structure of the highest pressure phase is controversial: we follow Zhang *et al.* [11] in refining it in the *Pnma* structure rather than the $C2/m$ adopted by Zhu *et al.* [12]. Rietveld refinements at 21.9 and 39.4 GPa (Fig. 2, right) indicate coexisting *Cmca* and *Pnma* phases and pure *Pnma* phase, respectively.

The $P2_1/c$ phase has a triple-layered Te (Ag)-Ag-Te (Ag) stacking structure, where the Te atoms occupy a distorted

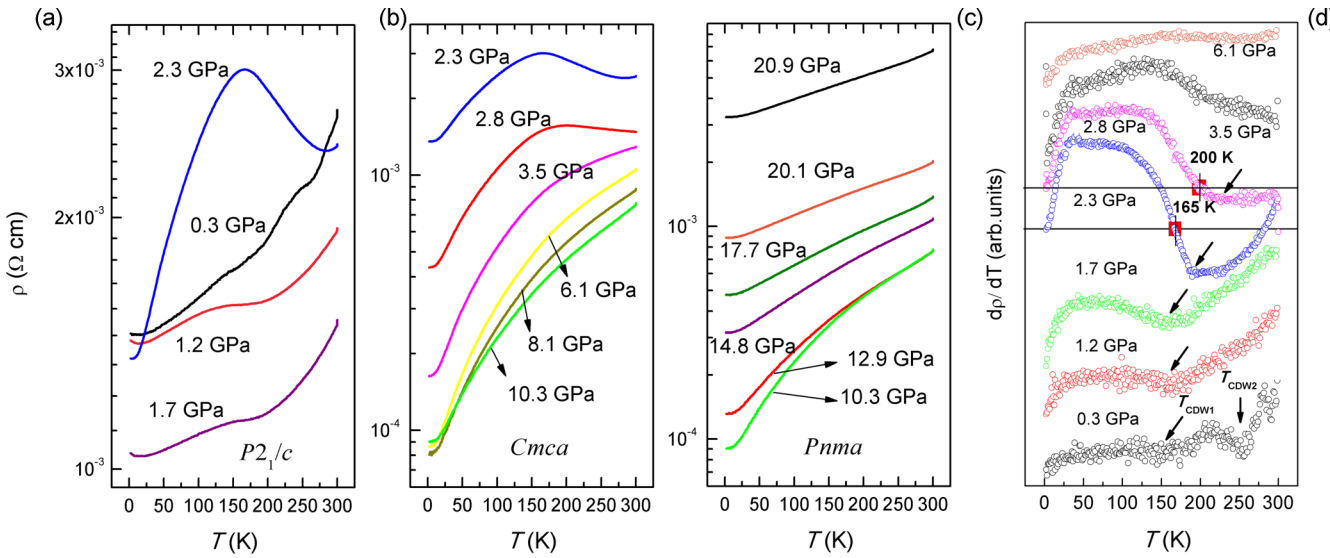

FIG. 3. (a)–(c) Resistivity versus temperature for different pressures at zero field. (d) The temperature derivative of the resistivity $d\rho/dT$; two turning points are seen at 0.3 GPa, denoted T_{CDW1} and T_{CDW2}. With increasing pressure T_{CDW1} can be observed up to 2.8 GPa while T_{CDW2} is no longer evident. The solid horizontal lines indicate points where $d\rho/dT = 0$ at 2.3 and 2.8 GPa.

fcc lattice with Ag atoms inserted in the interstitials. The centrosymmetric space group *Cmca* has an inversion center in the middle of two Te (Ag)-Ag-Te (Ag) triplets. The $TeAg_9$ coordination polyhedron chains undergo a shear glide when the *Cmca* phase transforms to *Pnma*. Lattice parameters derived from Rietveld fits at each measured pressure [Fig. 1(b)] indicate clearly the $P2_1/c \rightarrow Cmca$ transition at 2.9 GPa and the $Cmca \rightarrow Pnma$ transition at around 12.9 GPa. The inset showing the a/c lattice parameter ratio reveals a discontinuity between 1.9 and 2.3 GPa. Since the $P2_1/c$ structure is maintained through this transition, it must correspond to the electronic isostructural transition identified in previous work [11,12]. The unit-cell volume plotted in Fig. 1(c) shows discontinuities at the two structural phase transitions and the inset one at between 1.9 and 2.3 GPa due to the isostructural transition as in Ag_2Te. The Rietveld fit to the structural phase transition at 2.9 GPa shows coexisting $P2_1/c$ and *Cmca* phases present at this pressure. The value of the a/c shown in Fig. 1(b) corresponds to the $P2_1/c$ component.

To summarize, the crystal structure is the $P2_1/c$ phase between 0.3 and 2.9 GPa including an electronic isostructural transition around 2.1 GPa, the *Cmca* phase between 2.9 and about 12.9 GPa, and the *Pnma* phase between 12.9 and at least 43 GPa, with some admixture of *Cmca* at the lower-pressure end of this range.

B. Electronic transport

The resistivity versus temperature for various pressures at zero magnetic field is shown in Fig. 3. At lower pressures [Fig. 3(a)], $Ag_{2-\delta}Te$ generally displays behavior typical of a doped small-gap semiconductor, with resistivity rising with temperature since the carrier density is changing slowly and the phonon scattering increases with temperature. However, our $\rho(T)$ data from 0.3 to 1.7 GPa show features that are difficult to describe, even allowing the possibility that multiple bands participate in transport. The manifest break in the slope of $\rho(T)$, interrupting an overall metallic dependence, is reminiscent of a CDW transition. Also, above the isostructural transition, an overall increase in resistivity and emergence of an apparent thermally activated behavior further appear to indicate the opening of a gap. The CDW phase is attenuated with increasing pressure and totally suppressed, or possibly moved to temperatures above 300 K, above the $P2_1/c \rightarrow Cmca$ phase transition at 2.9 GPa [Fig. 3(b)]. Above this pressure the $\rho(T)$ curve shows metallic behavior, decreasing with pressure and then gradually increasing after the $Cmca \rightarrow Pnma$ transition at 12.9 GPa [Fig. 3(c)].

The onset of CDW ordering is already visible at 0.3 GPa as two kinks in the $\rho(T)$ curve just below room temperature, denoted T_{CDW1} and T_{CDW2} in the temperature $d\rho/dT$ in Fig. 3(d). Upon further increasing the pressure, T_{CDW2} is no longer evident and T_{CDW1} increases from 145 to 190 K at 2.3 GPa, in contrast to the decrease with pressure observed in $TbTe_3$ [16]. In contrast, this phenomenon is suppressed by pressure in $NbSe_3$ and $Ba_{1-x}R_xIrO_3$, in which a magnetic field enhances the resistance anomaly associated with the formation of the lower CDW state [17,18]. T_{CDW1} further increases to 235 K at 2.8 GPa and then is no longer evident.

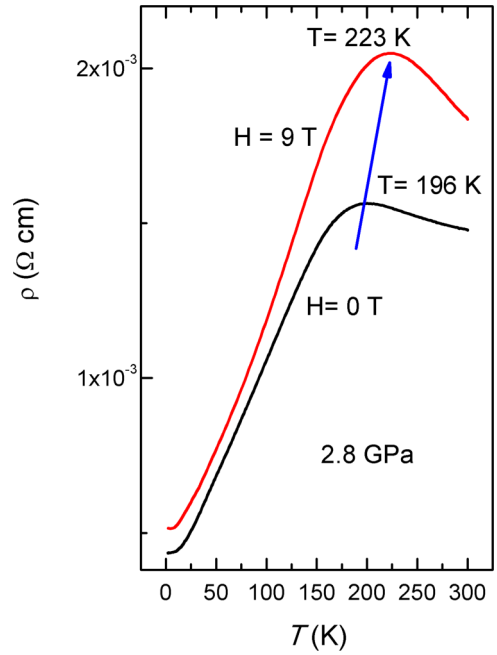

FIG. 4. Temperature dependence of the resistivity in magnetic fields $H = 9$ T and $H = 0$ T at 2.8 GPa. The curves are a guide to the eye.

Since we are unable to discern corresponding CDW features in the XRD data, we look to the magnetotransport data for further insight. Figure 4 shows the temperature dependence of the resistance at $H = 0$ and 9 T at 2.8 GPa. The application of a magnetic field enhances the $\rho(T)$ anomaly and the broad peak shifts from 196 K at $H = 0$ to 223 K at $H = 9$ T, implying that the electronic Zeeman energy is sufficient to alter the gapping of the Fermi surface as in $Ba_{1-x}R_xIrO_3$ [18].

The pressure dependence of the Hall resistivity ρ_{xy} as a function of magnetic field at different temperatures is shown in Fig. 5. The negative values of $\rho_{xy}(H)$ imply negative

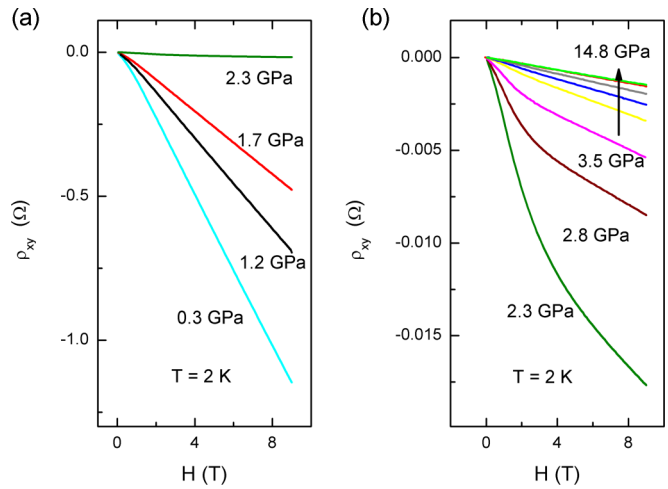

FIG. 5. (a), (b) Hall resistivity ρ_{xy} at 2 K as a function of magnetic field at different pressures and 2 K, showing that the dominant carriers are electrons. The Hall coefficient is nonlinear in the CDW phase between 2.3 and 3.5 GPa.

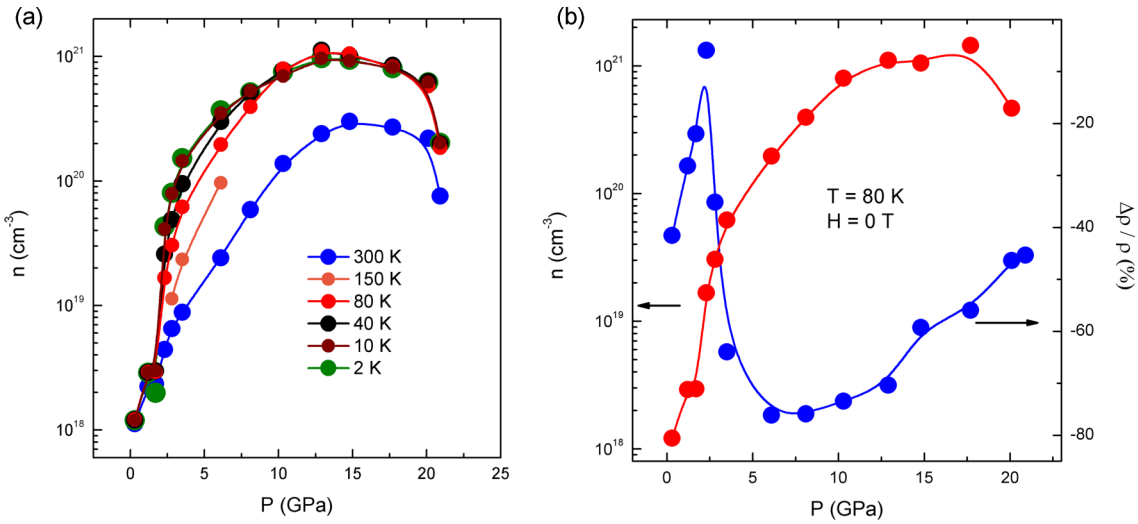

FIG. 6. (a) Pressure dependence of the carrier density n at different temperatures. (b) Pressure dependence of the relative change of resistivity with temperature, $\Delta\rho/\rho = [\rho(80\,\mathrm{K}) - \rho(300\,\mathrm{K})]/\rho(300\,\mathrm{K})$, showing an anomalous peak at 2.3 GPa, compared with the carrier density at 80 K. The curves are a guide to the eye.

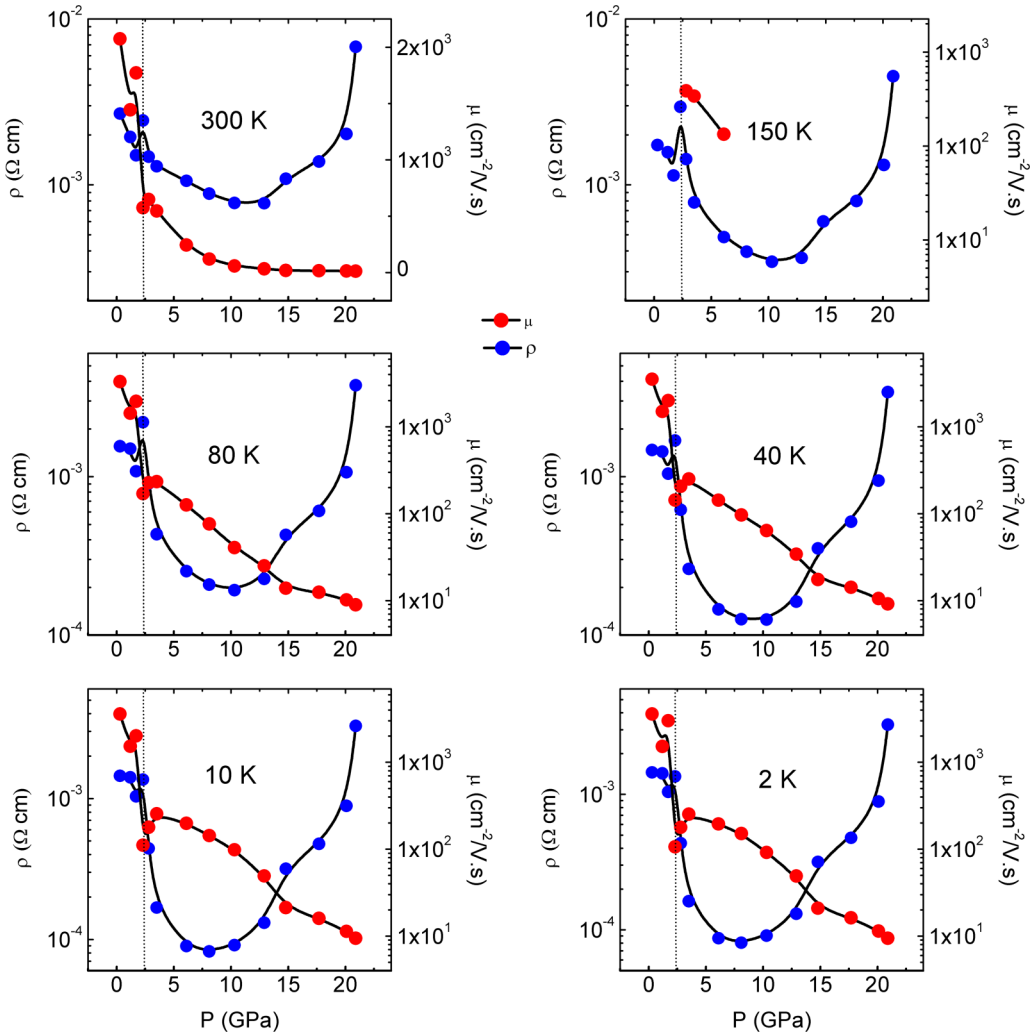

FIG. 7. Pressure dependence of resistivity ρ (blue points) and carrier mobility μ (red points) at different temperatures. The resistivity shows a singularity at 2.3 GPa, while the carrier mobility drops at the same pressure. The curves are a guide to the eye.

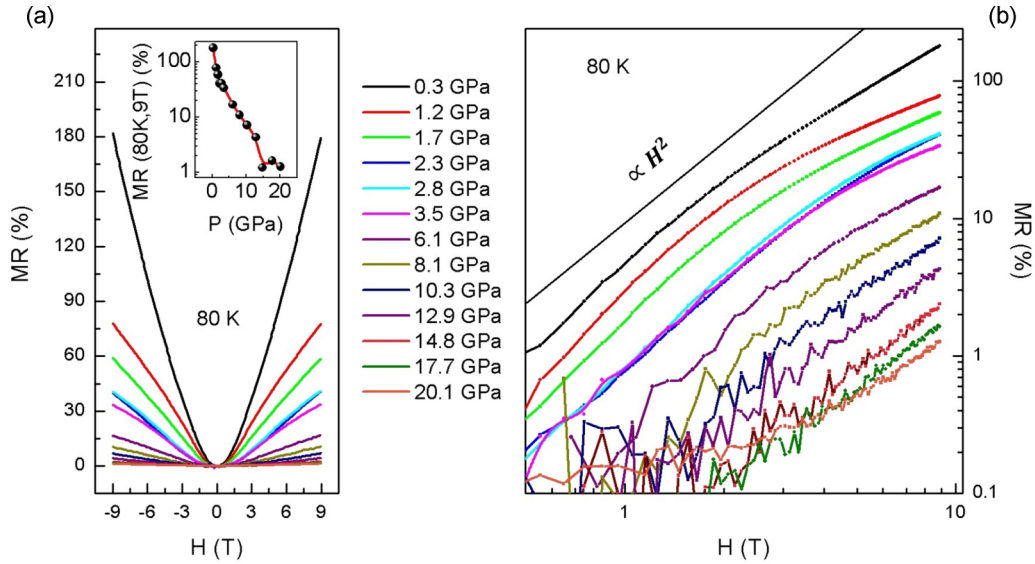

FIG. 8. Magnetoresistance for a series of pressures at 80 K shown as (a) a linear-linear plot and (b) a log-log plot. It exhibits quadratic behavior at low fields changing to a nonsaturating linear behavior at higher fields and is strongly reduced with increasing pressure, reverting to quadratic behavior over the measured field range above 10 GPa. The inset to (a) shows the MR at 9 T as a function of pressure at the same temperatures; the curve is a guide to the eye.

Hall coefficients R_H, indicating dominant electron transport; similar negative values were found by Schnyders at ambient pressure [13]. Between 2.3 and 3.5 GPa the Hall resistivity is nonlinear in the CDW phase. Assuming a single band, the carrier density [Fig. 6(a)] is estimated to be $n = 1/e|R_H| = 4.3\times10^{19}$ cm^{-3} at 2 K and 0.3 GPa. The pressure dependence of the relative change of resistivity with temperature, $\Delta\rho/\rho = [\rho(80\,\mathrm{K}) - \rho(300\,\mathrm{K})]/\rho(300\,\mathrm{K})$, shown at 80 K in Fig. 6(b), exhibits an anomalous peak at 2.3 GPa, where the carrier density is rising sharply. The pressure dependences of the resistivity $\rho(P)$ exhibits a peak at 2.3 GPa, especially evident at 80–300 K, and the mobility $\mu(P) = (ne\rho)^{-1}$ suddenly drops at the same pressure (Fig. 7). The MR shown in Fig. 8 for a series of pressures at 80 K exhibits quadratic behavior at low fields changing to a nonsaturating linear behavior at higher fields, and is strongly reduced with increasing pressure, reverting to quadratic behavior over the measured field range above 10 GPa.

At pressures below 1.9 GPa [Fig. 5(a)], the Hall resistivity is linear with field and diminishes with pressure while the average mobility is high and essentially pressure independent. This behavior could reasonably be explained by a dominant, high-mobility electron band being shifted downward through the Fermi level with pressure, a scenario supported by the diminished magnitude of the MR with pressure. However, the magnetotransport data also indicate dramatic band-structure changes at pressures above the isostructural transition. The previously linear Hall resistivity yields to curvature and, although bending to lower slope above 4 T, the subsequent linear increase still indicates dominant n-type carriers of much lower mobility. This could indicate the sudden reduction of the number of the high-mobility electrons, reversing the trend of steady increase of their number with pressure below 1.7 GPa, while revealing a second population of lower mobility electrons which correspond to the emergent activated behavior in $\rho(T)$. The MR echoes the same rapid elimination of the high-mobility carriers at 1.7 GPa by simultaneously transitioning to quadraticlike behavior of lower magnitude.

The increase in resistivity and emergence of apparent activated behavior at 2.3 GPa could be ascribed to isostructural-transition-induced changes in the band structure, but this would require us to ignore the features in $\rho(T)$ below the transition. The transition itself is by no means well understood, and we now briefly compare our data to the predictions implied by previously calculated band structures. The steady decrease in resistivity and generally metallic temperature dependencies of n-type Ag_2Te for pressures 0.3 to 1.7 GPa are in basic agreement with the band-structure predictions of Zhao *et al.* [10]. However, the emergent thermally activated behavior stands in apparent contradiction to the predictions of the same study, where a decrease in resistivity is predicted through the isostructural transition as the bands reconfigure and the gap appears to close. Our resistivity data seem even further from agreement with the band-structure calculations of Zhang *et al.* [11], which predict an opening bulk gap from 0.3 to 1.7 GPa, and a suddenly narrowed direct gap at the isostructural transition. Although we agree with both of these authors on the structure of the phases which form the basis of their band calculations, our electrical transport measurements appear to indicate that additional physics remains to be discerned.

Here we are proposing that a CDW exists in n-type Ag_2Te, minimally at pressures between 0.3 and 2.9 GPa and spanning the isostructural transition. It is possible that the isostructural transition strengthens the CDW or eliminates obscuring high-mobility carriers from the transport measurements.

We mention here briefly that measurements of the resistance in two different geometries [19] indicated metallic topological surface states [5,8,9] below 100 K. Since these

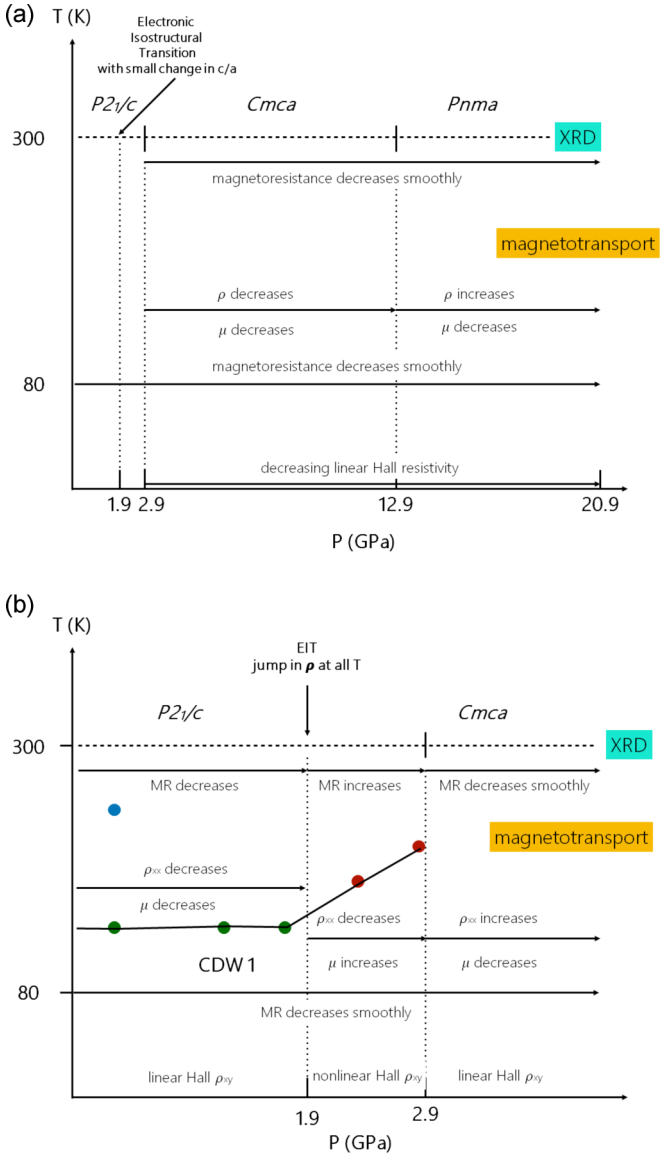

FIG. 9. Phase diagram of $Ag_{2-\delta}Te$ summarizing the structural and electronic transport results over (a) the full range from 0.4 to 20.9 GPa and (b) a restricted range highlighting the CDW behavior.

are not expected to be a factor in the results presented here, we defer discussion of them to a later paper.

A *P-T* phase diagram of $Ag_{2-\delta}Te$ with specific numbers of pressures for structural changes and CDW temperatures is presented in Fig. 9, to clarify the emergence of the CDW behavior with respect to other transitions.

IV. CONCLUSIONS

We have measured the structural and electronic properties of single-phase self-doped samples of $Ag_{2-\delta}Te$, free of a secondary metallic phase and with a well-characterized silver deficit, over extensive ranges of pressure, temperature, and magnetic field. In accord with previous work [10–12], we observe in these samples an isostructural transition around 2.1 GPa [Figs. 1(b) and 1(c)], structural phase transitions at 2.9 and around 12.9 GPa (Figs. 1 and 2), and a positive MR that is suppressed with increasing pressure (Fig. 8).

The most significant finding in this work is the observation of behavior that is already in evidence at 0.3 GPa is enhanced after the isostructural transition and is most pronounced at 2.3 GPa, where several anomalies are observed:

(1) a broad peak in the temperature dependence of the resistivity centered at 165 K, suggesting Fermi surface reconstruction (Fig. 3);

(2) a peak in the pressure dependence of the resistivity, especially pronounced in the relative change of resistivity with temperature [Fig. 6(b)];

(3) enhancement and shift to higher temperature following the application of a 9-T magnetic field, implying that the electronic Zeeman energy is sufficient to alter the gapping of the Fermi surface (Fig. 4);

(4) nonlinear dependence of the Hall resistivity on magnetic field [Fig. 5(b)]; and

(5) a sudden drop in the pressure dependence of the mobility (Fig. 7).

For reasons discussed in the previous section and from comparison with CDW phases reported in the literature, we are postulating that these anomalies are due to a CDW gapping at the Fermi surface.

We hope that these results will stimulate further theoretical work on the increasingly rich behavior discovered in nonstoichiometric silver chalcogenides.

ACKNOWLEDGMENTS

This work was financially supported by the National Nature Science Foundation of China (Grants No. 51527801 and No. U1530402). The HP-XRD experiments were conducted at HPCAT, which is supported by DOE-NNSA under Award No. DENA0001974 and DOE-BES under Award No. DE-FG02-99ER45775, with partial instrumentation funding by NSF. This research used resources of the Advanced Photon Source, a U.S. Department of Energy (DOE) Office of Science User Facility operated for the DOE Office of Science by Argonne National Laboratory under Contract No. DE-AC02-06CH11357.

[1] R. Xu, A. Husmann, T. F. Rosenbaum, M.-L. Saboungi, J. E. Enderby, and P. B. Littlewood, Nature (London) **390**, 57 (1997).

[2] H. S. Schnyders, M.-L. Saboungi, and T. F. Rosenbaum, Appl. Phys. Lett. **76**, 1710 (2000).

[3] A. Husmann, J. B. Betts, G. S. Boebinger, A. Migliori, T. F. Rosenbaum, and M.-L. Saboungi, Nature (London) **417**, 421 (2002).

[4] M. Lee, T. F. Rosenbaum, M.-L. Saboungi, and H. Schnyders, Phys. Rev. Lett. **88**, 066602 (2002).

[5] W. Zhang, R. Yu, W. Feng, Y. Yao, H. Weng, X. Dai, and Z. Fang, Phys. Rev. Lett. **106**, 156808 (2011).

[6] A. A. Abrikosov, Phys. Rev. B **58**, 2788 (1998).

[7] M. M. Parish and P. B. Littlewood, Phys. Rev. B **72**, 094417 (2005).

[8] A. Sulaev, P. Ren, B. Xia, Q. H. Lin, T. Yu, C. Qiu, S.-Y. Zhang, M.-Y. Han, Z. P. Li, W. G. Zhu, Q. Wu, Y. P. Feng, L. Shen, S.-Q. Shen, and L. Wang, AIP Adv. **3**, 032123 (2013).
[9] A. Sulaev, W. Zhu, K. L. Teo, and L. Wang, Sci. Rep. **5**, 8062 (2015).
[10] Z. Zhao, S. Wang, H. Zhang, and W. L. Mao, Phys. Rev. B **88**, 024120 (2013).
[11] Y. Zhang, Y. Li, Y. Ma, Y. Li, G. Li, X. Shao, H. Wang, T. Cui, X. Wang, and P. Zhu, Sci. Rep. **5**, 14681 (2015).
[12] J. Zhu, A. R. Oganov, W. X. Feng, Y. G. Yao, S. J. Zhang, X. H. Yu, J. L. Zhu, R. C. Yu, C. Q. Jin, X. Dai, Z. Fang, and Y. S. Zhao, AIP Adv. **6**, 085003 (2016).
[13] H. S. Schnyders, Appl. Phys. Lett. **107**, 042103 (2015).
[14] H. S. Schnyders (private communication).
[15] R. Andreaus and W. Sitte, J. Electrochem. Soc. **144**, 1040 (1997).
[16] J. J. Hamlin, D. A. Zocco, T. A. Sayles, M. B. Maple, J. H. Chu, and I. R. Fisher, Phys. Rev. Lett. **102**, 177002 (2009).
[17] S. Yasuzuka, Y. Okajima, S. Tanda, K. Yamaya, N. Takeshita, and N. Môri, Phys. Rev. B **60**, 4406 (1999).
[18] O. B. Korneta, S. Chikara, S. Parkin, L. E. DeLong, P. Schlottmann, and G. Cao, Phys. Rev. B **81**, 045101 (2010).
[19] C. Shekhar, C. E. ViolBarbosa, B. Yan, S. Ouardi, W. Schnelle, G. H. Fecher, and C. Felser, Phys. Rev. B **90**, 165140 (2014).